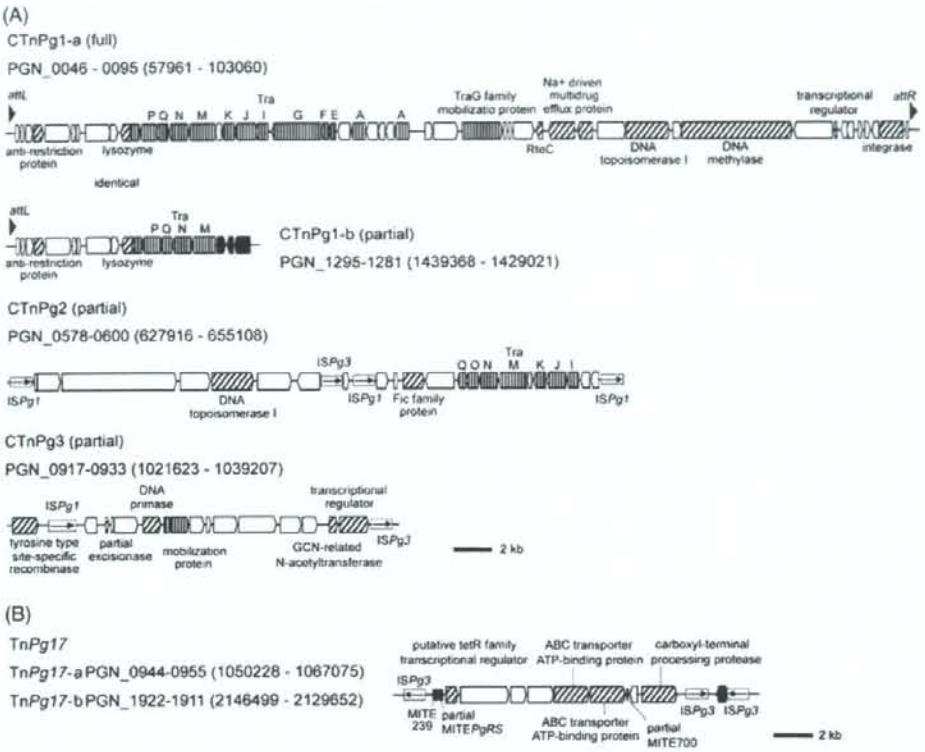

Figure 2. Novel CTns and Tn identified in the ATCC 33277 genome. (**A**) Structures of CTnPg1-a, CTnPg1-b, CTnPg2, and CTnPg3. (**B**) Structure of Tn*Pg17*. CDSs are depicted by arrows and IS elements by open boxes (vertically striped arrow, *tra* or *mob* genes; thin arrow in box, IS transposase; black arrow, partial transposase; hatched arrow, other functionally annotated CDS; white arrow, hypothetical protein). Black triangles in CTnPg1-a and CTnPg1-b indicate direct repeat sequences, and black boxes in Tn*Pg17* MITEs. The regions of CTnPg1-a and CTnPg1-b indicated by gray shading have an identical sequence.

Table 1. IS elements and MITEs on the ATCC 33277 and W83 genomes

Mobile genetic element	Strain	
	ATCC 33277 Number of intact copies (number of fragments)	W83[a] Number of intact copies (number of fragments)
IS*Pg1*	31 (18)	11 (40)
IS*Pg2*	2 (4)	5 (3)
IS*Pg3*	22 (7)	4 (5)
IS*Pg4*	0 (2)	10 (0)
IS*Pg5*	0 (4)	10 (1)
IS*Pg6*	0 (3)	1 (2)
IS*Pg7*	0 (0)	1 (0)
MITE239	12 (2)	5 (0)
MITE*PgRS*	11 (9)	14 (7)
MITE700	7 (7)	7 (2)

[a]Determined based on the reannotated W83 data.

that of IS*Pg3*. However, MITE700 and MITE464 exhibited highly variable structures, and their structural features have not been described in detail in the previous report.[19] Therefore, we first determined the structural features of these two MITEs by comparing the sequences of all of the MITE700 and MITE464 copies identified in ATCC 33277.

MITE700 also contains the same TIRs as those of IS*Pg3*, but its internal sequence is not related to that of MITE239. We identified 14 copies of MITE700 (including seven partial copies) in ATCC 33277. Multiple sequence alignment analysis revealed that MITE700 is ~720 bp in length but exhibits a high sequence variation due to internal deletions/insertions. The sequence of a region located just downstream of the left TIR is highly variable between the copies. We identified three subtypes of MITE700 based on the sequence variation in this region (Supplementary Fig. S1).

MITE464 has the same TIRs as those of IS*Pg1*. We found that its internal sequence consists of three types of repeat sequences (referred to as Repeats A, B, and C) (Fig. 3 and Supplementary Fig. S2). Repeats A and B exist just inside both TIRs, constituting a direct-repeat-like structure. Between the two Repeat A/B regions, multiple Repeat C regions exist in tandem, but the number of Repeat C regions varies between MITE464 copies, up to 14 repeats. Since no such repeating structure has been found in any MITEs described so far, we propose a new name for this MITE, MITE*PgRS* (MITE of *P. gingivalis* with Repeating Sequences).

On the basis of the structural features of each MITE, we rescreened IS elements and MITEs on the W83 genome, and we identified 93 IS elements (including 51 partial ones) and 35 MITEs (including nine partial ones) (Table 1 and Supplementary Table S7). The total numbers of IS elements and MITEs of the two strains were very similar, but the compositions showed a significant difference. In ATCC 33277, IS*Pg1*, IS*Pg3*, and MITE239 have been significantly expanded, whereas no intact copies of IS*Pg4* and IS*Pg5* are present. A previous study also showed that the numbers of copies and insertion sites of IS*Pg1* (formerly IS*1126*) markedly varied among *P. gingivalis* strains.[42] The composition of IS elements and MITEs may be an important feature to distinguish strains of *P. gingivalis*.

3.5. *Genome rearrangement*

Whole genome sequence alignment analysis by using the MUMmer program revealed that extensive genomic rearrangements have taken place between ATCC 33277 and W83 (Fig. 4). A number of X-shaped structures were observed, indicating that symmetrical inversions repeatedly occurred around the replication axis. We identified a total of 175 genomic regions in which genomic rearrangements took place in either strain. Inversions or translocations were observed in 35 regions, and simple insertions,

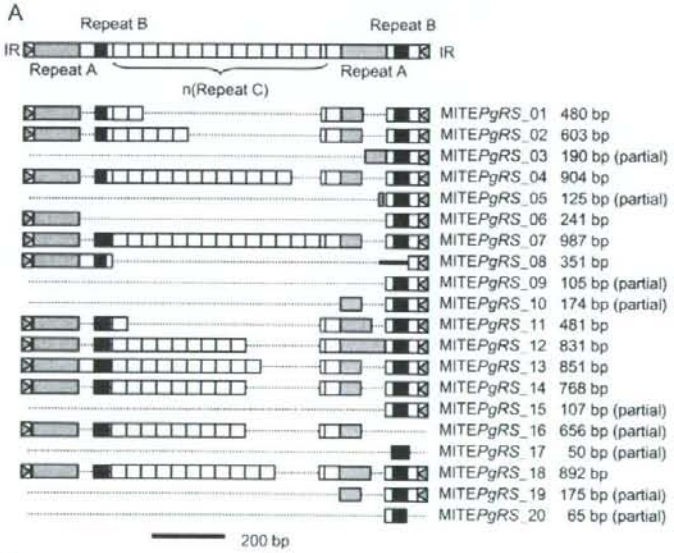

Figure 3. MITE in *P. gingivalis* with Repeating Structure (MITE*PgRS*). (**A**) Schematic presentation of the consensus structure of MITE*PgRS* and the structures of 20 copies of MITE*PgRS* identified in the ATCC 33277 genome are shown. Three kind of repeat sequences, Repeats A, B, and C, are depicted by colored boxes. Red triangles indicate IR sequences and a black thick line in MITE*PgRS*_08 a unique nucleotide sequence. (**B**) Consensus sequences of Repeats A, B, and C are shown.

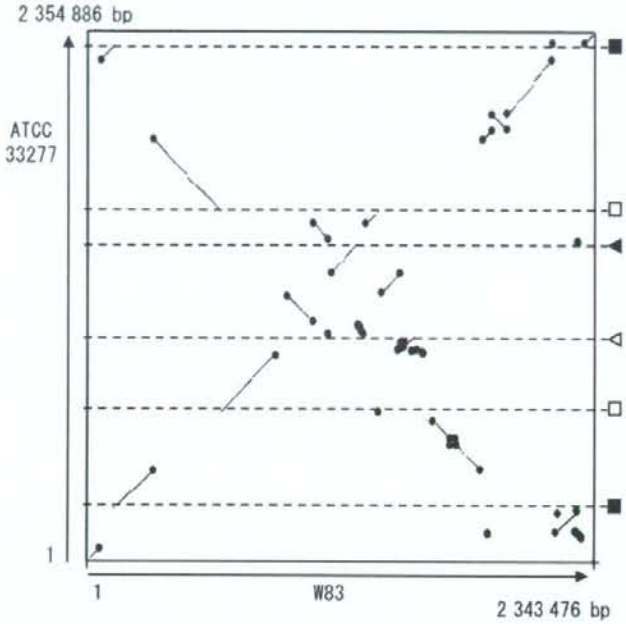

Figure 4. The DNA sequence identity plot of *P. gingivalis* ATCC 33277 and W83 chromosomes. The *dnaA* gene is located at the left and bottom corner. Black circles indicate mobile genetic elements (CTn Tn, IS, MITE, or a not-well-defined large mobile element of W83). The chromosomal locations of other genetic elements that mediated inversions or translocations are shown in the right: *rrn* operons (black squares), duplicated regions coding for a histone-like DNA binding protein, a hypothetical protein and elongation factor P (open squares), 12/13 bp repeat sequences (black triangle), and 11 bp repeat sequences (open triangle).

deletions, or replacements were observed in 140 regions. Remarkably, about two-thirds of these genomic rearrangements were associated with the presence of mobile genetic elements (IS, MITE, Tn, CTn, and a not well-defined large mobile element of W83). Large inversions or translocations have occurred between two *rrn* operons, duplicated DNA regions coding for a histone-like family DNA-binding protein (PGN_0614 and PGN_1407), a hypothetical protein (PGN_0615 and PGN_1406), elongation factor P (PGN_0616 and PGN_1405), two identical 11 bp sequences (TAATCATAATA), and two similar 12/13 bp sequences (TTTTC(GCC/AATG)AAAA). DNA sequences similar to the 12/13 bp sequences were also present in the *att* sites for CTn*Pg1* described in the following section. These rearrangements appear to be deeply involved in the generation of strain-specific CDSs: 60% of ATCC 33277-specific CDSs and 68% of W83-specific CDSs were created by these genomic rearrangements.

ATCC 33277 and W83 both contain four *rrn* operons of identical nucleotide sequences, but chromosomal locations of the four *rrn* operons differ markedly between the strains. By comparing the *rrn* operon-flanking regions in the two strains, we found that an inversion had taken place between *rrn1* and *rrn4* (see Supplementary Fig. S3). Additional genomic rearrangements that have occurred in the genomic loci other than *rrn* operons further altered the relative locations of the four *rrn* operons on the two genomes. We analyzed the structures of *rrn* operon-flanking regions in five other strains of *P. gingivalis* (TDC60, TDC117, TDC275, SU63, and GAI7802) using a set of orientation-specific primer pairs, and we found that all of the *rrn* operon-flanking regions of these five strains have the same structures as those of ATCC 33277 (Supplementary Fig. S3). This result suggests that inversions between *rrn1* and *rrn4* have taken place specifically in the W83 strain lineage among the strains tested.

The genomic regions for the biosynthesis of cell surface molecules have also significantly diverged between the two strains. They included the regions for FimA fimbrilin, Mfa1 fimbrilin, capsular polysaccharides, RagA and RagB antigens, and glycosyl transferase.[42–45] Among these, the difference in the locus for capsular polysaccharide biosynthesis (GP1 locus) is particularly important because capsular

polysaccharide is known to be one of the major virulence factors of *P. gingivalis*. The GP1 locus of ATCC 33277 (PGN_0223-PGN_0236) is identical to that reported for strain 381[43] except that one nonsense mutation was found in the PGN_0223-homolog of strain 381 (Supplementary Fig. S4).

The clustered regularly interspaced short palindromic repeats (CRISPR) locus also exhibits notable structural difference between the two strains. The numbers of repeats in the repeat/spacer region of the CRISPR-30-36 locus are 120 in ATCC 33277 and 23 in W83 (Fig. 5). The nucleotide sequences of the repeats are identical, but there is no homology in the spacer regions. A part of the CRISPR-associated gene (*cas*) encoding region has been replaced by very different sequences. Of interest is that the gene organization of the *cas*-encoding region of ATCC 33277 is nearly identical to that of *B. fragilis* YCH46 but very different from that of W83. The gene products also exhibit a high level of similarity of amino-acid sequences to those of *B. fragilis* YCH46. These results suggest that these genes may have been horizontally transferred between *P. gingivalis* and *B. fragilis*.

Among the bacterial species so far sequenced, *Bacteroides* species are phylogenically most closely related to *P. gingivalis*. However, two sequenced *B. fragilis* strains show no such extensive genomic rearrangement as seen in *P. gingivalis*.[40,46] *Shigella flexneri*, a pathogen for dysentery, contains a large number of IS elements and the bacterium has induced extensive genomic rearrangements among strains, which may create differences in virulence and epidemicity.[47,48] In *P. gingivalis*, the genomic rearrangements induced by IS and other mobile genetic elements may also have been involved in the generation of strain-to-strain difference in virulence. In this context, a recent finding that treatment of *P. gingivalis* cells with H_2O_2 induces expression of the IS*Pg1* transposase gene is noteworthy.[49] The fact that the number of copies of IS*Pg1* varies among *P. gingivalis* strains and the fact that IS*Pg1* is frequently associated with genome rearrangements suggest that oxidative stress-induced expression of the IS*Pg1* transposase gene results in transposition of IS*Pg1* that may mediate genomic rearrangements in *P. gingivalis*, and such rearrangements may contribute to the adaptation of *P. gingivalis* strains to an oxygen concentration-changeable environment in the gingival crevice.

3.6. *Excision of CTnPg1*

We could not exactly determine the attachment (*att*) site of CTnPg1 by comparing the genome sequences of ATCC 33277 and W83 because integration of CTnPg1-a has induced a genomic rearrangement and half of CTnPg1-b has been deleted. We therefore examined whether CTnPg1 can be excised from the chromosome and form a circular intermediate. By PCR analysis of the chromosomal DNA of ATCC 33277 using two primers targeting the left and right ends of CTnPg1 (Fig. 6A), we obtained a PCR product of 1500 bp in size (Fig. 6B). We further investigated whether a cast-off genome can be generated by the excision of CTnPg1

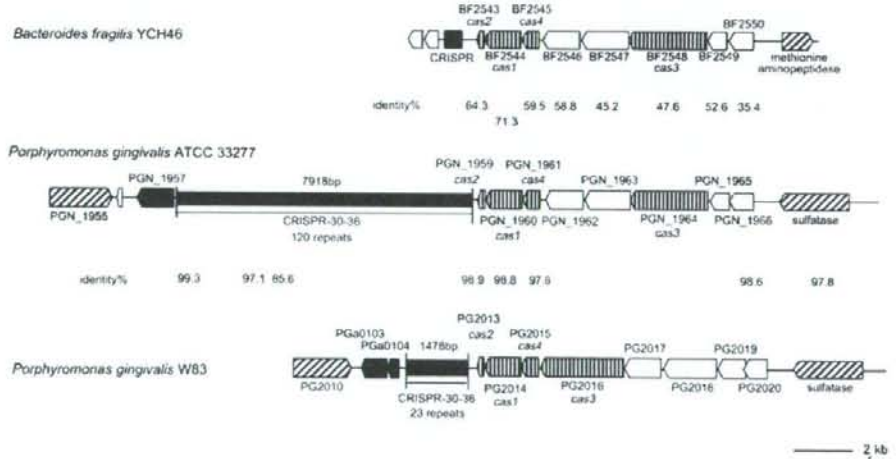

Figure 5. Comparison of CRISPR-30-36 regions of *P. gingivalis* and *B. fragilis*. Locations and directions of CDSs (arrows) and repeat regions (black rectangles) are drawn to scale. Homologous CDSs are indicated by gray shading, and their amino-acid sequence identities are also shown. CDSs for IS transposases are indicated by black arrows, *cas* genes by vertically striped arrows, other functionally annotated CDSs by hatched arrows, and CDSs for hypothetical proteins by white arrows. The identity between PGN_1964 and PG2016 is 15.7%.

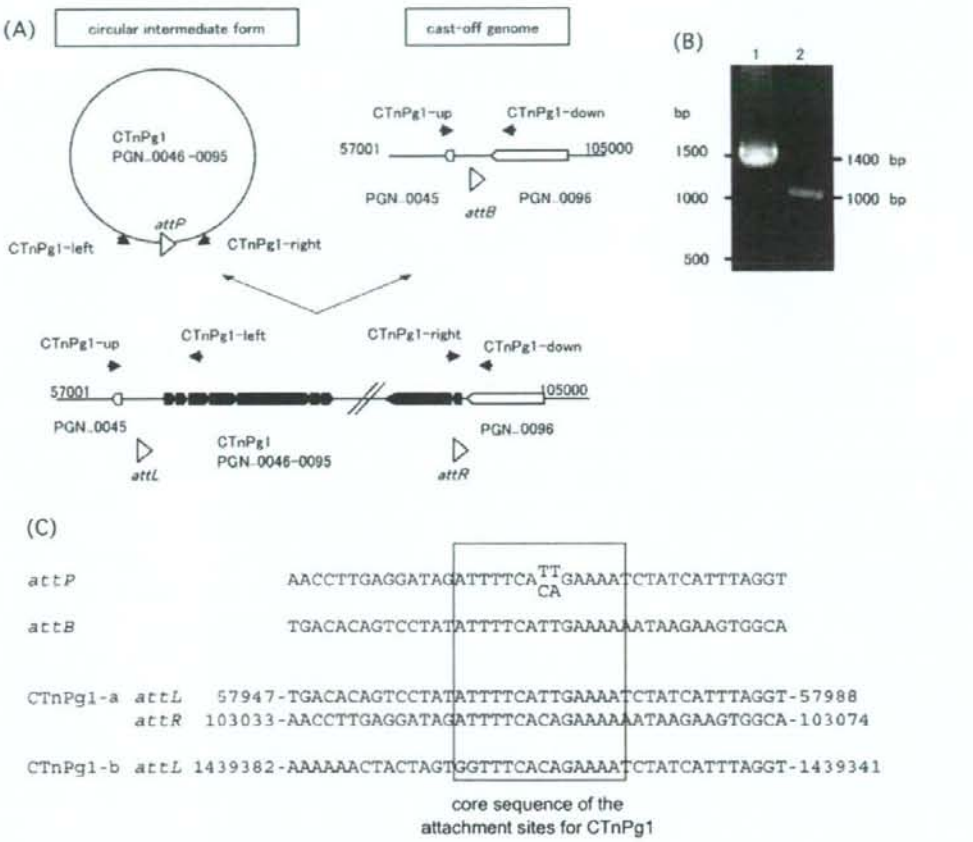

Figure 6. Excision of CTnPg1-a. (**A**) Schematic presentation of the structure of CTnPg1-a and the strategy to detect the excised circular intermediate and cast-off chromosome. Locations of PCR primers are indicated by black arrow heads. CDSs on CTnPg1 are depicted by black arrows and other CDSs by open arrows. Open triangles indicate *att* regions of CTnPg1. (**B**) Agarose gel electrophoresis of PCR products obtained by the primer pairs CTnPg1-right/CTnPg1-left (lane 1) and CTnPg1-up/CTnPg1-down (lane 2). (**C**) Sequence alignment of *attP*, *attB*, *attL*, and *attR* regions of CTnPg1. The 14 bp core sequence is indicated by a box.

using two PCR primers targeting the CTnPg1-a-flanking regions, and we obtained a PCR product of 1000 bp in size (Fig. 6A and B). By comparing the sequences of the two PCR products with the genome sequence of ATCC 33277, we identified the core sequence of the *att* site for CTnPg1, ATTTTCA(CA/TT)GAAAA (Fig. 6C). The same sequence was also found at one end of CTnPg1-b.

3.7. Glucose kinase-encoding gene

Disability of saccharolysis is one of the major characteristics of *P. gingivalis*. Consistent with this, the glucose kinase-encoding gene (*glk*) (PG1737) has a nonsense mutation in strain W83 (Supplementary Fig. S5). Nelson et al.[19] suggested that the defect of *glk* accounts for asaccharolysis of *P. gingivalis*. In ATCC 33277, the *glk* gene (PGN_0380) has also been disrupted by an insertion of MITE239 but contains no nonsense mutation. Therefore, we analyzed the *glk* genes of other *P. gingivalis* strains to know which type of genetic defect is generally observed in *P. gingivalis*. Unexpectedly, however, the *glk* genes of five strains examined (strains TDC60, TDC117, TDC275, SU63, and GAI7802) were all intact. We detected no nonsense mutation or MITE239 insertion although a few amino-acid substitutions were observed in these *glk* genes (Supplementary Fig. S5B). To determine whether the *glk* gene is expressed in the five strains, we quantified the mRNA of the *glk* gene using the

Kgp-encoding gene (*kgp*) as a control (Supplementary Table S8). In this analysis, a large amount of the *glk* gene transcript was detected in all of the five strains. On the other hand, all the strains used in this study (ATCC 33277, W83, and five other strains) were confirmed to be asaccharolytic (data not shown). Thus, these data suggest that defects of *glk*, which were detected in W83 and ATCC 33277, cannot always account for asaccharolysis of *P. gingivalis*. Further work is needed to clarify physiological roles of glucose kinase in *P. gingivalis* and what is responsible for asaccharolysis of *P. gingivalis*.

3.8. *Conclusion*

In this study, we determined the whole genome sequence of ATCC 33277, a less-virulent *P. gingivalis* strain, and carried out a genomic comparison with a virulent strain, W83. Although the genome size and GC content are almost the same, we detected extensive rearrangements between the two strains, many of which have been induced by various mobile genetic elements (IS, MITE, Tn, and CTn). Such structural alterations of the *P. gingivalis* genomes generated many strain-specific CDSs and may be closely associated with difference in virulence of the two strains.

Acknowledgements: We thank K. Oshima, K. Furuya, C. Yoshino, H. Inaba, K. Motomura, and Y. Hattori (University of Tokyo), A. Tamura and N. Itoh (Kitasato University), and Y. Kikuchi (Matsumoto Dental College) for their technical support.

Supplementary Data: Supplementary data are available online at www.dnaresearch.oxfordjournals.org.

Funding

This work was supported by Grants-in-Aid for Scientific Research on Priority Areas "Comprehensive Genomics" (No. 17020007) to M.H.; "Applied Genomics" (No. 18018032) to K.N. from the Ministry of Education, Culture, Sports, Science and Technology of Japan.

References

1. Papapanou, P. N. 1999, Epidemiology of periodontal diseases: an update, *J. Int. Acad. Periodontol.*, **1**, 110–116.
2. Irfan, U. M., Dawson, D. V. and Bissada, N. F. 2001, Epidemiology of periodontal disease: a review and clinical perspectives, *J. Int. Acad. Periodontol.*, **3**, 14–21.
3. Armitage, G. C. 1996, Periodontal diseases: diagnosis, *Ann. Periodontol.*, **1**, 37–215.
4. Oliver, R. C., Brown, L. J. and Loe, H. 1998, Periodontal diseases in the United States population, *J. Periodontol.*, **69**, 269–278.
5. Mattila, K. J., Valtonen, V. V., Nieminen, M. and Huttunen, J. K. 1995, Dental infection and the risk of new coronary events: prospective study of patients with documented coronary artery disease, *Clin. Infect. Dis.*, **20**, 588–592.
6. Beck, J., Garcia, R., Heiss, G., Vokonas, P. S. and Offenbacher, S. 1996, Periodontal disease and cardiovascular disease, *J. Periodontol.*, **67**, 1123–1137.
7. Joshipura, K. J., Rimm, E. B., Douglass, C. W., Trichopoulos, D., Ascherio, A. and Willett, W. C. 1996, Poor oral health and coronary heart disease, *J. Dent. Res.*, **75**, 1631–1636.
8. Morrison, H. I., Ellison, L. F. and Taylor, G. W. 1999, Periodontal disease and risk of fatal coronary heart and cerebrovascular diseases, *J. Cardiovasc. Risk*, **6**, 7–11.
9. Chiu, B. 1999, Multiple infections in carotid atherosclerotic plaques, *Am. Heart J.*, **138**, S534–S536.
10. Kozarov, E. V., Dorn, B. R., Shelburne, C. E., Dunn, W. A. Jr and Progulske-Fox, A. 2005, Human atherosclerotic plaque contains viable *Actinbacillus actinomycetemcomitans* and *Porphyromonas gingivalis*, *Arterioscler. Thromb. Vasc. Biol.*, **25**, e17–e18.
11. Boone, D. R. and Castenholtz, R. W. 2002. *Bergey's Manual of Systematic Bacteriology*, 2nd Ed., Vol. 1., Springer-Verlag: New York.
12. Mayrand, D. and Holt, S. C. 1988, Biology of asaccharolytic black-pigmented Bacteroides species, *Microbiol. Rev.*, **52**, 134–152.
13. Lamont, R. J. and Jenkinson, H. F. 1998, Life below the gum line: pathogenic mechanisms of *Porphyromonas gingivalis*, *Microbiol. Mol. Biol. Rev.*, **62**, 1244–1263.
14. Holt, S. C., Kesavalu, L., Walker, S. and Genco, C. A. 1999, Virulence factors of *Porphyromonas gingivalis*, *Periodontology*, **20**, 168–238.
15. Amano, A. 2007, Disruption of epithelial barrier and impairment of cellular function by *Porphyromonas gingivalis*, *Front. Biosci.*, **12**, 3965–3974.
16. Umemoto, T. and Hamada, N. 2003, Characterization of biologically active cell surface components of a periodontal pathogen: the roles of major and minor fimbriae of *Porphyromonas gingivalis*, *J. Periodontol.*, **74**, 119–122.
17. Kadowaki, T., Nakayama, K., Okamoto, K., et al. 2000, *Porphyromonas gingivalis* proteinases as virulence determinants in progression of periodontal diseases, *J. Biochem.*, **128**, 153–159.
18. Slots, J. and Rams, E. T. 1993, Pathogenicity. In: Shah, H. N., Mayrand, D. and Genco, R. J. (eds.), *Biology of the Species Porphyromonas gingivalis*, CRC Press Inc.: Boca Raton, FL, pp. 127–131.
19. Nelson, K. E., Fleischmann, R. D., DeBoy, R. T., et al. 2003, Complete genome sequence of the oral pathogenic Bacterium *Porphyromonas gingivalis* strain W83, *J. Bacteriol.*, **185**, 5591–5601.
20. Nakayama, K. 1994, Rapid viability loss on exposure to air in a superoxide dismutase-deficient mutant of

Porphyromonas gingivalis, *J. Bacteriol.*, **176**, 1939–1943.
21. Nakayama, K., Kadowaki, T., Okamoto, K. and Yamamoto, K. 1995, Construction and characterization of arginine-specific cysteine proteinase (Arg-gingipain)-deficient mutants of *Porphyromonas gingivalis*: evidence for significant contribution of Arg-gingipain to virulence, *J. Biol. Chem.*, **270**, 23619–23626.
22. Okamoto, K., Nakayama, K., Kadowaki, T., Abe, N., Ratnayake, D. B. and Yamamoto, K. 1998, Involvement of a lysine-specific cysteine proteinase in hemoglobin adsorption and heme accumulation by *Porphyromonas gingivalis*, *J. Biol. Chem.*, **273**, 21225–21231.
23. Shi, Y., Ratnayake, D. B., Okamoto, K., Abe, N., Yamamoto, K. and Nakayama, K. 1999, Genetic analyses of proteolysis, hemoglobin binding, and hemagglutination of *Porphyromonas gingivalis*: construction of mutants with a combination of *rgpA*, *rgpB*, *kgp*, and *hagA*, *J. Biol. Chem.*, **274**, 17955–17960.
24. Naito, M., Sakai, E., Shi, Y., et al. 2006, *Porphyromonas gingivalis*-induced platelet aggregation in plasma depends on Hgp44 adhesin but not Rgp proteinase, *Mol. Microbiol.*, **59**, 152–167.
25. Watanabe-Kato, T, Hayashi, JI, Terazawa, Y, et al. 1998, Isolation and characterization of transposon-induced mutants of *Porphyromonas gingivalis* deficient in fimbriation, *Microb. Pathog.*, **24**, 25–35.
26. Ewing, B. and Green, P. 1998, Base-calling of automated sequencer traces using Phred. II. Error probabilities, *Genome Res.*, **8**, 186–194.
27. Gordon, D., Desmarais, C. and Green, P. 2001, Automated finishing with autofinish, *Genome Res.*, **11**, 614–625.
28. Nakayama, K. 1995, Determination of the genome size of the oral anaerobic bacterium *Porphyromonas gingivalis* by pulsed field gel electrophoresis, *Dent. Jpn.*, **32**, 25–28.
29. Sakiyama, T., Takami, H., Ogasawara, N., et al. 2000, An automated system for genome analysis to support microbial whole-genome shotgun sequencing, *Biosci. Biotechnol. Biochem.*, **64**, 670–673.
30. Badger, J. H. and Olsen, G. J. 1999, CRITICA: coding region identification tool invoking comparative analysis, *Mol. Biol. Evol.*, **16**, 512–524.
31. Yada, T., Nakao, M., Totoki, Y. and Nakai, K. 1999, Modeling and predicting transcriptional units of *Escherichia coli* genes using hidden Markov models, *Bioinformatics*, **15**, 987–993.
32. Frishman, D., Mironov, A., Mewes, H. W. and Gelfand, M. 1998, Combining diverse evidence for gene recognition in completely sequenced bacterial genomes, *Nucleic Acids Res.*, **26**, 2941–2947.
33. Altschul, S. F., Madden, T. L., Schaffer, A. A., et al. 1997, Gapped BLAST and PSI-BLAST: a new generation of protein database search programs, *Nucleic Acids Res.*, **25**, 3389–3402.
34. Lowe, T. M. and Eddy, S. R. 1997, tRNAscan-SE: a program for improved detection of transfer RNA genes in genomic sequence, *Nucleic Acids Res.*, **25**, 955–964.
35. Delcher, A. L., Phillippy, A., Carlton, J. and Salzberg, S. L. 2002, Fast algorithms for large-scale genome alignment and comparison, *Nucleic Acids Res.*, **30**, 2478–2483.
36. Schwartz, S., Zhang, Z., Frazer, K. A., et al. 2000, PipMaker—a web server for aligning two genomic DNA sequences, *Genome Res.*, **10**, 577–586.
37. Pfaffl, M. W. 2001, A new mathematical model for relative quantification in real-time RT–PCR, *Nucleic Acids Res.*, **29**, e45.
38. Bacic, M., Parker, A. C., Stagg, J., et al. 2005, Genetic and structural analysis of the *Bacteroides* conjugative transposon CTn341, *J. Bacteriol.*, **187**, 2858–2869.
39. Bonheyo, G., Graham, D., Shoemaker, N. B. and Salyers, A. A. 2001, Transfer region of a bacteroides conjugative transposon, CTnDOT, *Plasmid*, **45**, 41–51.
40. Kuwahara, T., Yamashita, A., Hirakawa, H., et al. 2004, Genomic analysis of *Bacteroides fragilis* reveals extensive DNA inversions regulating cell surface adaptation, *Proc. Natl. Acad. Sci. USA*, **101**, 14919–14924.
41. Feschotte, C., Jiang, N. and Wessler, S. R. 2002, Plant transposable elements: where genetics meets genomics, *Nat. Rev. Genet.*, **3**, 329–341.
42. Dong, H., Chen, T., Dewhirst, F. E., Fleischmann, R. D., Fraser, C. M. and Duncan, M. J. 1999, Genomic loci of the *Porphyromonas gingivalis* insertion element IS1126, *Infect. Immun.*, **67**, 3416–3423.
43. Aduse-Opoku, J., Slaney, J. M., Hashim, A., et al. 2006, Identification and characterization of the capsular (K-antigen) locus of *Porphyromonas gingivalis*, *Infect. Immun.*, **74**, 449–460.
44. Fujiwara, T., Morishima, S., Takahashi, I. and Hamada, S. 1993, Molecular cloning and sequencing of the fimbrilin gene of *Porphyromonas gingivalis* strains and characterization of recombinant proteins, *Biochem. Biophys. Res. Commun.*, **197**, 241–247.
45. Hall, L. M., Fawell, S. C., Shi, X., et al. 2005, Sequence diversity and antigenic variation at the rag locus of *Porphyromonas gingivalis*, *Infect. Immun.*, **73**, 4253–4262.
46. Cerdeno-Tarraga, A. M., Patrick, S., Crossman, L. C., et al. 2005, Extensive DNA inversions in the *B. fragilis* genome control variable gene expression, *Science*, **307**, 1463–1465.
47. Nie, H., Yang, F., Zhang, X., et al. 2006, Complete genome sequence of *Shigella flexneri* 5b and comparison with *Shigella flexneri* 2a, *BMC Genomics*, **7**, 173.
48. Wei, J., Goldberg, M. B., Burland, V., et al. 2003, Complete genome sequence and comparative genomics of *Shigella flexneri* serotype 2a strain 2457T, *Infect. Immun.*, **71**, 2775–2786.
49. Diaz, P. I., Slakeski, N., Reynolds, E. C., Morona, R., Rogers, A. H. and Kolenbrander, P. E. 2006, Role of *oxyR* in the oral anaerobe *Porphyromonas gingivalis*, *J. Bacteriol.*, **188**, 2454–2462.

RESEARCH ARTICLE

$CD4^+$ T-cell activation by antigen-presenting cells infected with urease-deficient recombinant *Mycobacterium bovis* bacillus Calmette-Guérin

Tetsu Mukai, Yumi Maeda, Toshiki Tamura, Yuji Miyamoto & Masahiko Makino

Department of Microbiology, Leprosy Research Center, National Institute of Infectious Diseases, Tokyo, Japan

Correspondence: Masahiko Makino, Department of Microbiology, Leprosy Research Center, National Institute of Infectious Diseases, 4-2-1 Aobacho, Higashimurayama, Tokyo 189-0002, Japan. Tel.: +81 42 391 8059; fax: +81 42 391 8212; e-mail: mmaki@nih.go.jp

Received 22 November 2007; revised 11 February 2008; accepted 15 February 2008. First published online 9 April 2008.

DOI:10.1111/j.1574-695X.2008.00407.x

Editor: Patrick Brennan

Keywords
BCG; urease; macrophage; dendritic cell.

Abstract

We constructed a recombinant *Mycobacterium bovis* bacillus Calmette-Guérin (BCG-ΔUT) that lacks urease, providing acidic intraphagosomal conditions to drive an effective human immune T-cell response. BCG-ΔUT-infected macrophages stimulated autologous $CD4^+$ T cells more efficiently than parent BCG-infected macrophages. For further T-cell activation, BCG-ΔUT-infected macrophages required pretreatment with exogenous recombinant granulocyte-macrophage colony-stimulating factor or costimulation with either CD40 ligand or interferon-γ. By contrast, BCG-ΔUT-infected dendritic cells induced significant activation of naïve $CD4^+$ T cells without costimulating signals. C57BL/6 mice intradermally inoculated with BCG-ΔUT more efficiently produced memory T cells that responded to recall antigen. Therefore, the depletion of urease from BCG is useful for the activation of T cells.

Introduction

Mycobacteria, such as *Mycobacterium leprae* and *Mycobacterium tuberculosis*, are representative parasitic intracellular pathogens. *Mycobacterium leprae* is a causative agent of human leprosy, in cases of which skin lesions and chronic progressive peripheral nerve injury are usually observed (Stoner, 1979; Job, 1989). At present, around one-third of individuals are infected with *M. tuberculosis* and several millions die as result of tuberculosis each year (Dye *et al.*, 2005; World Health Organization, 2006). *Mycobacterium bovis* bacillus Calmette-Guérin (BCG) has been used as a vaccine against leprosy, although its efficacy is quite limited (Andersen & Doherty, 2005; Setia *et al.*, 2006). The emergence of multidrug-resistant strains of these mycobacteria is of concern (Maeda *et al.*, 2001; Kai *et al.*, 2004; Kaufmann, 2005), and therefore the urgent development of a new vaccine, including a more efficacious recombinant BCG, is desired (Kaufmann, 2005).

Among various immunocompetent cells, $CD4^+$ T cells, especially IFN-γ-producing cells, play an extremely important role in inhibiting the multiplication of mycobacteria, killing them in the early stages of infection, and keeping the bacterial load at a stable level (Orme *et al.*, 1993; Dockrell *et al.*, 1996; Hashimoto *et al.*, 2002). $CD4^+$ T cells that can respond quickly to pathogenic mycobacteria and produce IFN-γ are known as memory T cells. The efficient production of such memory T cells needs pre-exposure to antigenic vaccinating molecules, which share their antigenicity with that of pathogenic mycobacteria (Kaufmann, 2006). BCG has been considered a good candidate for a vaccine against *M. leprae* in this respect, however its efficacy is limited in several aspects, including the ability to activate T cells (Kaufmann & McMichael, 2005). BCG resides in the phagosomes of macrophages and thus attenuates the trafficking of antigenic molecules to the macrophage cell surface (Grode *et al.*, 2005). One possible strategy for improving the ability of BCG to stimulate T cells is to enhance its ability to fuse with the lysosomes. To this end, we knocked out the *urease* gene from BCG. The urease-deficient recombinant BCG (BCG-ΔUT) is expected to allow phagosomal acidification in the host cells, and induce efficient phagosome maturation for cytolytic activity of the antigenic molecules of BCG (Schaible *et al.*, 1998; Honerzu Bentrup & Russell, 2001).

In the present study, we evaluated the ability of BCG-ΔUT to activate IFN-γ-producing type 1 $CD4^+$ T cells through

© 2008 Federation of European Microbiological Societies
Published by Blackwell Publishing Ltd. All rights reserved

antigen-presenting cells (APCs), and to produce memory CD4$^+$ T cells. When used as a target of BCG-ΔUT, macrophages fully stimulated CD4$^+$ T cells in the presence of costimulatory agents such as CD40 ligand (L) and IFN-γ. In addition, BCG-ΔUT-infected monocyte-derived dendritic cells (DCs) activated type 1 CD4$^+$ T cells more efficiently than parent BCG-infected cells in the absence of these costimulators. Therefore, BCG-ΔUT was found to be a useful T-cell-stimulating agent.

Materials and methods

Preparation of blood cells

Peripheral blood was obtained from healthy purified protein derivative (PPD)-positive individuals with informed consent. PPD-negative individuals provide more information, however, as healthy individuals are PPD-positive, due to compulsory BCG vaccination for children in Japan (0–4 years old). Peripheral blood mononuclear cells (PBMCs) were isolated using Ficoll-Paque Plus (Pharmacia, Uppsala, Sweden) and cryopreserved in liquid nitrogen until use, as previously described (Makino & Baba, 1997). For the preparation of peripheral monocytes, CD3$^+$ T cells were removed from either freshly isolated heparinized blood, or cryopreserved PBMCs using immunomagnetic beads coated with anti-CD3 monoclonal antibody (mAb) (Dynabeads 450, Dynal, Oslo, Norway). The CD3$^-$ PBMC fraction was plated on collagen-coated plates and nonadherent cells were removed by extensive washing. The remaining adherent cells were used as monocytes (Makino & Baba, 1997). Macrophages were generated by culturing monocytes in the presence of 20% fetal calf serum and recombinant (r) macrophage colony-stimulating factor (M-CSF) (R&D Systems, Abingdom, UK) (Makino *et al.*, 2007). Macrophages were pulsed with rBCGs on day 5 of culture, and were used as a stimulator of T cells on day 7 (Makino *et al.*, 2007). Monocyte-derived DCs were differentiated as described previously (Makino *et al.*, 1999). Briefly, monocytes were cultured in the presence of 50 ng recombinant granulocyte-macrophage colony-stimulating factor (GM-CSF; Pepro Tech EC Ltd, London, UK) and 10 ng of recombinant interleukin (rIL)-4 (Pepro Tech) per millilitre (Makino *et al.*, 1999). On day 3 of culture, immature DCs were infected with rBCGs at the indicated multiplicity of infection (MOI), and on day 5 of culture, DCs were used for further analyses of surface antigens and for mixed-lymphocyte assays.

BCG culture and DNA manipulation

The mycobacterial strain, BCG substrain Tokyo, for DNA manipulation was grown in Middlebrook 7H9 broth (Difco Laboratories) with 0.05% Tween 80 or Middlebrook 7H10 agar (Difco) with 0.5% glycerol, each supplemented with 10% albumin–dextrose–catalase enrichment (Difco). DNA manipulations including isolation of DNA, transformation and PCR, were carried out as described previously (Miyamoto *et al.*, 2004). *Escherichia coli* strain DH5α was used for routine manipulation and the propagation of plasmid DNA. *Escherichia coli* strain STBL4 was used for the construction of plasmid vectors derived from phAE87. Antibiotics were added as required: hygromycin B, 150 μg mL^{-1} for *E. coli* and 75 μg mL^{-1} for *Mycobacterium smegmatis* (mc^{2}155) and *M. bovis* BCG. A recombinant BCG that lacks a *urease* gene was constructed. The sequence of the targeted gene, *ureC* (BCG 1886), was obtained from the BCG list (http://genolist.pasteur.fr/BCGList/). The *ureC* gene was inactivated by inserting a hygromycin-resistance cassette (*hyg*) using a specialized transducing phage system for homologous recombination (Bardarov *et al.*, 2002; Miyamoto *et al.*, 2006). To construct the disrupted sequence, fragments of around 0.9 kb both upstream and downstream of *ureC* were amplified from BCG-Tokyo genomic DNA using the following two pairs of primers: F UureC and R UureC for upstream of *ureC*, and F DureC and R DureC for downstream of *ureC*. The PCR products were digested with each restriction enzyme and cloned into the corresponding site flanking *hyg* of pYUB854 to give pYUB854-ureC-UD. This plasmid was used for packaging into the phasmid vector phAE87 to construct a specialized transducing mycobacteriophage for gene disruption as described previously (Bardarov *et al.*, 2002; Miyamoto *et al.*, 2006). BCG-Tokyo infected with the mycobacteriophage at an MOI of 50 was incubated at 37 °C for 3 h in 7H9 broth without Tween 80. Harvested bacterial cells were then plated and cultured on 7H10 agar containing hygromycin B (75 μg mL^{-1}) for 3 weeks. The hygromycin B-resistant colonies were selected and evaluated with a conventional urease assay. A change in the color of the assay medium from yellowish to red was scored as urease-positive. Furthermore, genomic DNA obtained from these colonies was subjected to PCR to confirm the disruption of the gene using primers F ureC and R ureC (Fig. 1). The colony which tested negative in the urease assay was named BCG-ΔUT, while the parental BCG substrain Tokyo is referred to as BCG-Tokyo.

Preparation of *M. leprae*

Mycobacterium leprae (Thai-53) was isolated from the footpads of BALB/c-*nu/nu* mice (McDermott-Lancaster *et al.*, 1987). The isolated bacteria were counted by Shepard's method (Charles & Shepard, 1960). The MOI for infection to host cells was determined based on the assumption that macrophages and DCs were equally susceptible to infection with BCG or *M. leprae* (Hashimoto *et al.*, 2002).

© 2008 Federation of European Microbiological Societies
Published by Blackwell Publishing Ltd. All rights reserved

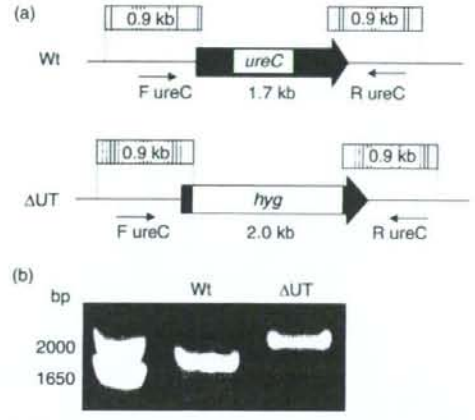

Fig. 1. Disruption of the *ureC* gene. (a) Schematic diagram of the *ureC* region on the chromosome of the wild-type *Mycobacterium bovis* BCG Tokyo strain and its gene disruptant, ΔUT. The shaded boxes indicate the regions included in the recombinant phage for gene disruption. The black arrow represents the coding region of the *ureC* gene. The gray box represents the hygromycin-resistace cassette (*hyg*). The primers used for PCR analysis are indicated by small arrows. (b) PCR analysis of the wild-type and the disruptant using the primers indicated above.

Preparation of mycobacterial antigen

The cytosolic fraction of BCG-Tokyo (BCC) was obtained as described previously (Maeda *et al.*, 2003). Briefly, the mycobacterial suspension containing the protease inhibitors was mixed with zirconium beads at a ratio of *c.* 1 : 1 (v/v) and homogenized using a Beads Homogenizer Model BC-20 (Central Scientific Commerce, Tokyo). The suspension was centrifuged at 10 000 ***g*** to remove the cell-wall fractions. The supernatant was then ultracentrifuged at 100 000 ***g*** and the resulting supernatant was taken as the cytosolic fraction. For preparation of the *M. leprae* membrane (MLM) fraction, *M. leprae* was used instead of BCG and treated similarly. The pellet obtained by ultracentrifugation (100 000 ***g*** for 1 h) was used as a membrane fraction (MLM). The optimal concentration of BCC and MLM for stimulating T cells was determined in advance.

Analysis of cell surface antigens

The expression of cell surface antigens on macrophages and DCs, either untreated or treated with exogenous rIFN-γ (R&D Systems), was analyzed using a FACSCalibur flow cytometer. Dead cells were eliminated from the analysis by staining with propidium iodide (Sigma Chemical Co., St. Louis, MO), and 1×10^4 live cells were analyzed. For the analysis of cell surface antigens, the following mAbs were used: fluorescein isothiocyanate (FITC)-conjugated mAbs against HLA-ABC (G46-2.6), HLA-DR (L243), CD14 (M5E2), CD40 (5C3) and CD86 (FUN-1). These mAbs were obtained from BD PharMingen (San Diego, CA).

APC function of rBCG-infected macrophages and DCs

The ability of rBCG-infected macrophages to stimulate T cells was assessed using an autologous mixed-lymphocyte assay as previously described (Wakamatsu *et al.*, 1999; Hashimoto *et al.*, 2002). The responder $CD4^+$ T cells were purified from freshly thawed PBMCs by using a CD4-negative isolation kit (Dynabeads 450; Dynal) (Wakamatsu *et al.*, 1999). The purity of $CD4^+$ T cells was more than 95% as assessed by fluorescence-activated cell sorting (FACS) analysis. Naïve $CD4^+$ T cells were produced by further treatment of $CD4^+$ T cells with an mAb to CD45RO antigen, followed by incubation with beads coated with goat antimouse IgG. Memory-type T cells were similarly produced by the treatment of cells with an mAb to CD45RA antigen. The purified responder cells (1×10^5 well^{-1}) were plated in 96-well round-bottom tissue culture plates and macrophages or DCs were added to give the indicated APC/$CD4^+$ T-cell ratio. Supernatants of the cocultures were collected on day 4 and the concentration of cytokines was determined. In some cases, macrophages were treated with the indicated dose of exogenous rGM-CSF (Pepro Tech) in advance of infection with rBCGs. Further, macrophages were infected with rBCGs in the presence of neutralizing mAb to IL-10 (JES3-9D7; Rat IgG, BD PharMingen) or control normal rat IgG. Macrophages infected with BCGs were further costimulated with either rCD40L (Pepro Tech) or rIFN-γ (R&D Systems), and in some cases, the macrophages were stimulated with rIFN-γ in the presence of anti-IFN-γ receptor α chain (CD119) (GIR-208, mouse IgG1, BD PharMingen) or control normal mouse IgG. In other cases, macrophages infected with BCG-ΔUT in the presence of exogenous rIFN-γ were treated with either mAb to HLA-DR (L243, mouse IgG2a), CD86 (IT2.2, mouse IgG2b, BD PharMingen) or control normal mouse IgG, and subsequently cocultured with responder $CD4^+$ T cells. The concentration of IFN-γ produced by $CD4^+$ T cells was quantified using an enzyme assay kit [OptEIA Human enzyme linked immunosorbent assay (ELISA) Set; BD Biosciences].

Production of IL-12p70 and IL-1β by DCs

The ability of DCs to produce IL-12p70 and IL-1β on stimulation with BCG-Tokyo or BCG-ΔUT was assessed. The DCs were stimulated with BCGs at the indicated MOI for 24 h, and the concentration of these cytokines was quantified using the Opt EIA Human ELISA Set.

© 2008 Federation of European Microbiological Societies
Published by Blackwell Publishing Ltd. All rights reserved

Animal studies

For inoculation into mice, BCG-Tokyo and BCG-ΔUT were cultured in Middlebrook 7H9 to log phase and stored at 10^8 CFU mL^{-1} at −80 °C. Before aliquots were used for inoculation, the concentration of viable bacilli was determined by plating cells on the Middlebrook 7H10 agar plate. Three 5-week-old C57BL/6J mice per group were inoculated intradermally with 0.1 mL phosphate-buffered saline (PBS) containing 1×10^2 or 1×10^3 BCG-Tokyo or BCG-ΔUT. The animals were kept under specific pathogen-free conditions and were supplied with sterilized food and water. Four weeks after injection, the spleens were removed, and the splenocytes were suspended at a concentration of 2×10^6 cells mL^{-1} in culture medium, and stimulated with the indicated concentration of BCC or MLM in triplicate in 96-well round-bottomed microplates. The individual culture supernatants were collected 3 days after stimulation, and IFN-γ and IL-2 were measured using an OptEIA mouse ELISA set.

Statistical analysis

The Student's *t*-test was applied to determine statistical differences.

Results

Induction of the fusion of BCG-ΔUT-infected phagosomes with lysosomes

The efficacy with which BCG-ΔUT-infected phagosomes fused with lysosomes in macrophages was examined using confocal microscopy. Lysosomes were stained with anti-LAMP1 mAb after treatment of THP-1 cells with FITC-labeled BCG-Tokyo or BCG-ΔUT for 24 h. The parental BCG colocalized with lysosomes less efficiently than BCG-ΔUT (data not shown). Therefore, BCG-ΔUT may at least partially enhance the ability to induce phagosomal maturation.

T-cell-stimulating activity of BCG-ΔUT

The activity of BCG-ΔUT to stimulate IFN-γ-producing CD4$^+$ T cells, when infected to macrophages, was assessed (Fig. 2). BCG-ΔUT-infected macrophages activated unseparated CD4$^+$ T cells to release IFN-γ substantially more efficiently than parent BCG-infected macrophages. Although BCG-ΔUT-infected macrophages also induced production of IL-2 from CD4$^+$ T cells (data not shown), the extent of IFN-γ (< 50 pg mL^{-1}) and IL-2 production was not as high as expected. Furthermore, BCG-ΔUT did not induce the activation of naïve CD4$^+$ T cells (data not shown). As the activation of T cells is largely influenced by the cytokine milieu, in which T cells and their stimulators

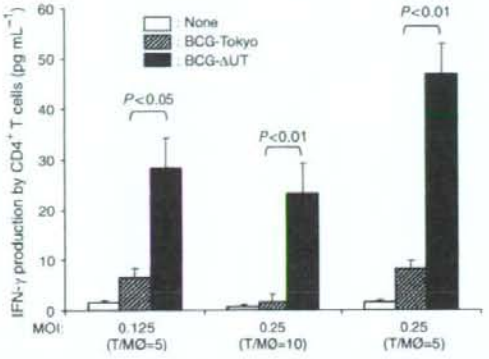

Fig. 2. Production of IFN-γ by CD4$^+$ T cells. Macrophages, differentiated by 5 days of culture with rM-CSF from monocytes, were infected with BCG-Tokyo (parental BCG) or BCG-ΔUT at the indicated MOI, and cultured for another 2 days in the presence of rM-CSF. These macrophages were used as a stimulator of autologous CD4$^+$ T cells (1×10^5 cells well^{-1}) at the indicated T-cell/macrophage ratio in a 4-day culture. A representative example of three separate experiments is shown. Assays were performed in triplicate and the results are expressed as the means ± SD. Titers were statistically compared using Student's *t*-test.

are present, we determined the level of cytokines produced from macrophages on stimulation with BCG-ΔUT. BCG-ΔUT produced significantly more cytokines, such as IL-10, GM-CSF, TNFα and IL-1β, than the parental BCG (data not shown). It has been reported that IL-10 inhibits the APC-mediated activation of T cells (Granelli-Piperno *et al.*, 2004) and GM-CSF regulates the function of macrophages (Makino *et al.*, 2007). To examine the role of IL-10 on T-cell activation, macrophages were infected with BCGs in the presence of a neutralizing mAb to IL-10 (Fig. 3a). The IFN-γ production by stimulated CD4$^+$ T cells was not influenced by the treatment of macrophages with control IgG; however, a significantly higher level of IFN-γ was produced on treatment with the neutralizing mAb to IL-10. The up-regulation by IL-10 mAb treatment was observed in both BCG-Tokyo and BCG-ΔUT in a similar fashion. Furthermore, the pretreatment of macrophages with exogenous GM-CSF also significantly upregulated the antigen-presenting function of macrophages, although the effect of GM-CSF was more pronounced in BCG-ΔUT-infected macrophages (Fig. 3b).

Next, we phenotypically assessed the effect of BCG-ΔUT on macrophages (Fig. 4a). BCG-ΔUT induced enhanced expression of both CD14 and CD40 on macrophages compared with BCG-Tokyo. Based on these results, we treated BCG-infected macrophages with CD40L to examine its role as a costimulator of macrophages (Fig. 4b). The CD40L treatment upregulated the T-cell activation by BCG-

© 2008 Federation of European Microbiological Societies
Published by Blackwell Publishing Ltd. All rights reserved

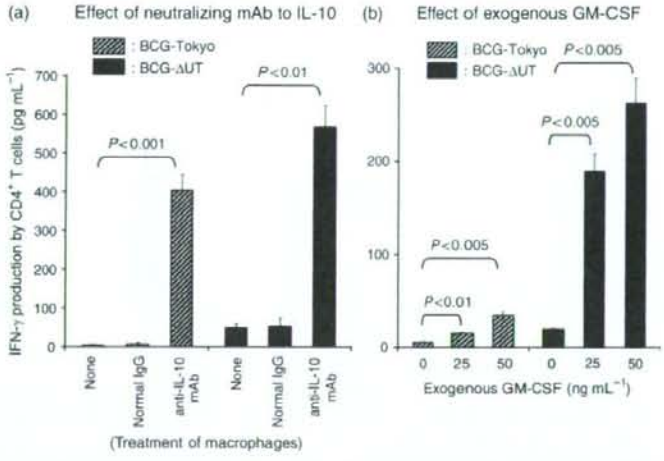

Fig. 3. Effect of IL-10 and GM-CSF on IFN-γ production. (a) Macrophages differentiated from monocytes by using rM-CSF were infected with either BCG-Tokyo or BCG-ΔUT at an MOI of 0.25 on day 5 of culture and cultured for another 2 days in the presence of rM-CSF. The BCG-infected macrophages were treated with neutralizing mAb to IL-10 or isotype-matched control IgG (10 μg mL^{-1}), and used as a stimulator of CD4$^+$ T cells, at a T-cell/macrophage ratio of 10 : 1, and cultured for another 4 days. The optimal concentration of mAb was determined in advance. (b) Macrophages obtained by 4 days of culture with rM-CSF were treated with the indicated dose of rGM-CSF. The macrophages pretreated with rGM-CSF were infected with BCG-Tokyo or BCG-ΔUT at an MOI of 0.25, cultured for another 2 days in the presence of rM-CSF used as a stimulator of CD4$^+$ T cells on day 8, at a T-cell/macrophage ratio of 10 : 1 (4 days of stimulation). A representative example of three separate experiments is shown. Assays were performed in triplicate and the results are expressed as the means ± SD. Titers were statistically compared using Student's *t*-test.

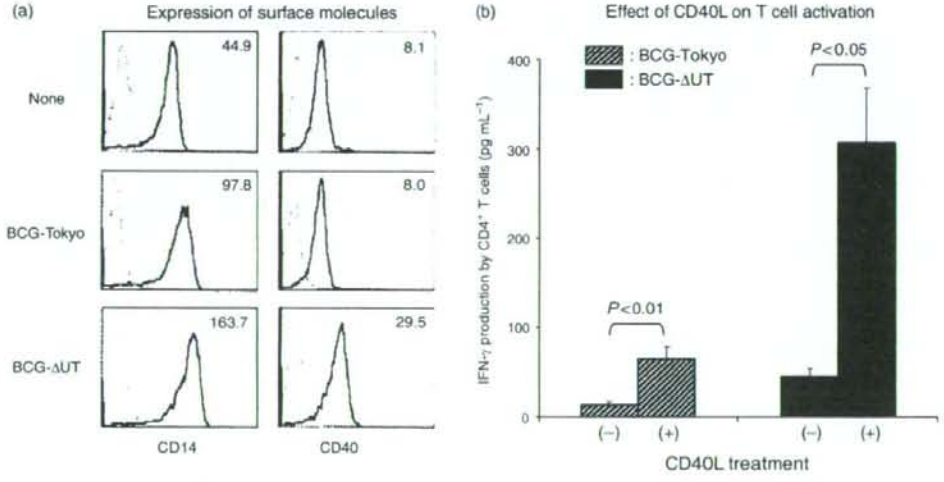

Fig. 4. (a) Expression of CD14 and CD40 molecules on macrophages. Macrophages produced by using rM-CSF were infected with BCGs at an MOI of 0.25, and cultured for another 2 days in the presence of rM-CSF. The macrophages on day 7 of culture were gated and analyzed. Dotted lines, isotype-matched control IgG; solid lines, the indicated test mAb. The number in the top right-hand corner of each panel represents the difference in mean fluorescence intensity between the control IgG and the test mAb. Representative results of three separate experiments are shown. (b) IFN-γ production by CD4$^+$ T cells stimulated with BCG-infected macrophages. Macrophages differentiated from monocytes using rM-CSF were infected with BCGs at an MOI of 0.25 on day 5 of culture, further treated with CD40L (1 μg mL^{-1}) on day 6, and used as a stimulator of CD4$^+$ T cells (T-cell/macrophage ratio of 10 : 1, 4 days of stimulation). A representative of three separate experiments is shown. Assays were performed in triplicate and the results are expressed as the means ± SD. Titers were statistically compared using Student's *t*-test.

© 2008 Federation of European Microbiological Societies
Published by Blackwell Publishing Ltd. All rights reserved

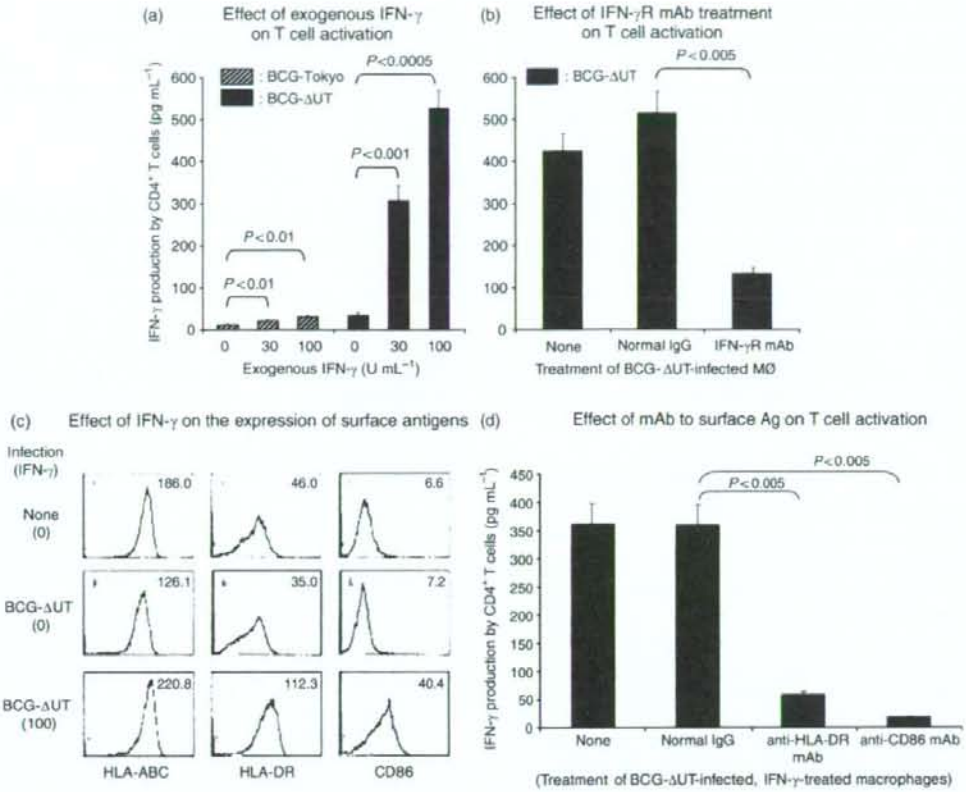

Fig. 5. (a) Effect of exogenous IFN-γ on CD4+ T-cell activation. Macrophages produced by 5 days of culture with rM-CSF from monocytes were infected with BCGs at an MOI of 0.25 and simultaneously treated with the indicated dose of exogenous IFN-γ. The macrophages were used as a stimulator of CD4+ T cells (T-cell/macrophage ratio of 10 : 1, 4 days of stimulation). A representative of three separate experiments is shown. Assays were performed in triplicate and the results are expressed as the means ± SD. Titers were statistically compared using Student's *t*-test. (b) Involvement of IFN-γ receptor in T-cell activation. Macrophages produced as in (a) were infected with BCG-ΔUT (MOI of 0.25), stimulated with exogenous IFN-γ (100 U mL^{-1}) in the presence of mAb to IFN-γ receptor α-chain (CD119) or isotype matched control IgG (10 μg mL^{-1}), and cultured for another 2 days in the presence of rM-CSF. The macrophages were used as a stimulator of CD4+ T cells (T-cell/macrophage ratio of 10 : 1, 4 days of stimulation). A representative of three separate experiments is shown. Assays were performed in triplicate and the results are expressed as the means ± SD. Titers were statistically compared using Student's *t*-test. (c) Surface expression of various molecules on BCG-ΔUT-infected, IFN-γ-treated macrophages. Macrophages produced as in (a) were infected with BCG-ΔUT (MOI of 0.25), stimulated with exogenous IFN-γ (100 U mL^{-1}) and cultured for another 2 days in the presence of rM-CSF. The macrophages on day 7 of culture were gated and analyzed. Dotted lines, isotype-matched control IgG; solid lines, the indicated test mAb. The number in the top right-hand corner of each panel represents the difference in mean fluorescence intensity between the control IgG and the test mAb. Representative results of three separate experiments are shown. (d) Involvement of surface antigens of BCG-ΔUT-infected, IFN-γ-stimulated macrophages in T-cell activation. Macrophages produced as in (a) were infected with BCG-ΔUT (MOI of 0.25), treated with exogenous IFN-γ (100 U mL^{-1}) and cultured for another 2 days in the presence of rM-CSF. These macrophages were cocultured with autologous CD4+ T cells at a T-cell/macrophage ratio of 10 : 1 in a 4-day culture in the presence of the indicated mAb (10 μg mL^{-1}). A representative of three separate experiments is shown. Assays were performed in triplicate and the results are expressed as the means ± SD. Titers were statistically compared using Student's *t*-test.

infected macrophages, but it more efficiently affected BCG-ΔUT-infected macrophages. Similarly, there was a significant difference between parent BCG and BCG-ΔUT in sensitivity to IFN-γ (Fig. 5a). However, other cytokines such as TNFα and IL-1β did not enhance the T-cell-stimulating activity of rBCG-infected macrophages. The IFN-γ treatment was effective against both BCG-Tokyo- and BCG-ΔUT-infected macrophages; however, more than a 10-fold increase in the production of IFN-γ from T cells was achieved only when BCG-ΔUT-infected macrophages

© 2008 Federation of European Microbiological Societies
Published by Blackwell Publishing Ltd. All rights reserved

were stimulated with exogenous IFN-γ. The optimal stimulation of T cells induced the production of more than 500 pg mL^{-1} IFN-γ. The exogenous IFN-γ seems to contribute directly to the enhancement of APC function, as the IFN-γ-mediated enhancement was cancelled out by the pretreatment of BCG-ΔUT-infected macrophages with mAb to IFN-γ receptor α-chain (Fig. 5b). Furthermore, IFN-γ significantly enhanced the expression of HLA-DR and CD86 on BCG-ΔUT-infected macrophages (Fig. 5c), while the phenotypic alteration of BCG-Tokyo-infected macrophages by IFN-γ was minimum (data not shown). When BCG-ΔUT-infected, IFN-γ-treated macrophages were treated with mAb to either HLA-DR or CD86 in advance of being cocultured with CD4$^+$ T cells, IFN-γ production by the T cells was significantly inhibited, while normal murine IgG treatment did not have any effect (Fig. 5d).

CD4$^+$ T-cell activation by BCG-ΔUT-infected DCs

As BCG-ΔUT significantly but less efficiently activated CD4$^+$ T cells through macrophages in the absence of costimulation, the potency of BCG-ΔUT-infected DCs as a T-cell activator was evaluated. Expression of surface molecules on DCs infected with either BCG-Tokyo or BCG-ΔUT was examined (Fig. 6a). Expression of HLA-ABC, HLA-DR, CD86 and CD83 was more significantly upregulated by the infection with BCG-ΔUT than with BCG-Tokyo. Higher levels of IL-12p70 and IL-1β were produced by BCG-ΔUT stimulation (Fig. 6b). Furthermore, we assessed whether BCG-ΔUT activated naïve and memory CD4$^+$ T cells through DCs by using various MOI titers and multiple T/DC ratios (Fig. 6c). IFN-γ levels were significantly higher following stimulation with BCG-ΔUT than with parent BCG in both naïve and memory CD4$^+$ T cells. Also, a higher level of CD40L was expressed on CD4$^+$ T cells after stimulation with BCG-ΔUT-infected DCs (data not shown). These results indicate that the infection of DCs with BCG-ΔUT alone was sufficient, as compared with macrophages which required costimulators to drive a strong T-cell response.

Memory T-cell production by BCG-ΔUT

Another important aspect of using BCG as a vaccine is the production of memory T cells *in vivo*. We examined the response of splenic T cells obtained from BCG-infected C57BL/6 mice to mycobacterial recall antigen (Fig. 7). We used BCC as a recall antigen. At 4 weeks following infection, splenic T cells from BCG-ΔUT-infected mice produced more IFN-γ than those from mice infected with BCG-Tokyo by responding to BCC. The lymphocyte population producing IFN-γ was found to be CD4$^+$ T cells by intracellular staining (data not shown). Furthermore, upon stimulation with MLM, which contains immunodominant antigens of *M. leprae*, CD4$^+$ T cells from BCG-ΔUT-infected mice produced significantly higher levels of IFN-γ than those from uninfected or BCG-Tokyo-infected mice (Fig. 7).

Discussion

To date, BCG is the only suitable vaccine against leprosy; however, its efficacy is quite limited. Overall efficacy in one meta-analysis was reported to be only 26% (Setia *et al.*, 2006). Several reasons might explain why BCG cannot block multiplication of *M. leprae* or inhibit the development of leprosy. The most important defect of BCG is that it is retained in phagosomes of macrophages, avoiding phagosomal acidification and hence interfering in the efficient fusion of BCG-containing phagosomes with lysosomes (Clements *et al.*, 1995; Reyrat *et al.*, 1995; Grode *et al.*, 2005). The lack of phagosome–lysosome fusion inhibits the trafficking of BCG-derived antigens through the major histocompatibility class (MHC) II pathway, which is enrolled for preferential stimulation of CD4$^+$ T cells, the most important cells involved in inhibition of *M. leprae* growth (Sendide *et al.*, 2004). Further, macrophages produce abundant amounts of IL-10 on infection with BCG, which, in turn, inhibits the activation of CD4$^+$ T cells (Mochida-Nishimura *et al.*, 2001; Granelli-Piperno *et al.*, 2004).

In the present study, we constructed a recombinant BCG (BCG-ΔUT) that lacks a *urease* gene through allelic exchange of chromosomal DNA. As urease is involved in the maintenance of intraphagosomal pH at neutral (Grode *et al.*, 2005) or slightly alkaline values (Sendide *et al.*, 2004), lack of this enzyme may contribute to the induction of phagosomal acidification (Sendide *et al.*, 2004), thereby promoting the fusion of BCG-containing phagosomes with lysosomes. The efficient colocalization of BCG-ΔUT with lysosome was observed, leading us to expect an efficient enhancement of T-cell activation by BCG-ΔUT-infected macrophages. Previously, rBCG deficient in urease C was produced by a similar system and found to be superior to parental BCG in producing acidic conditions (pH 4.5–5.5) in BCG-infected phagosomes in murine macrophages (Reyrat *et al.*, 1995; Grode *et al.*, 2005). However, it was not demonstrated whether the rBCG deficient in urease C promoted the MHC class II trafficking pathway and actually activated human CD4$^+$ T cells through APCs. The newly constructed BCG-ΔUT lacked urease activity and *in vitro* studies confirmed that it could not degrade urea to ammonia. When BCG-ΔUT was infected to macrophages, it activated human CD4$^+$ T cells more efficiently than the parental BCG. However, the amount of IFN-γ released from the T cells was not as high as expected (< 50 pg mL^{-1}). These results suggest that

© 2008 Federation of European Microbiological Societies
Published by Blackwell Publishing Ltd. All rights reserved

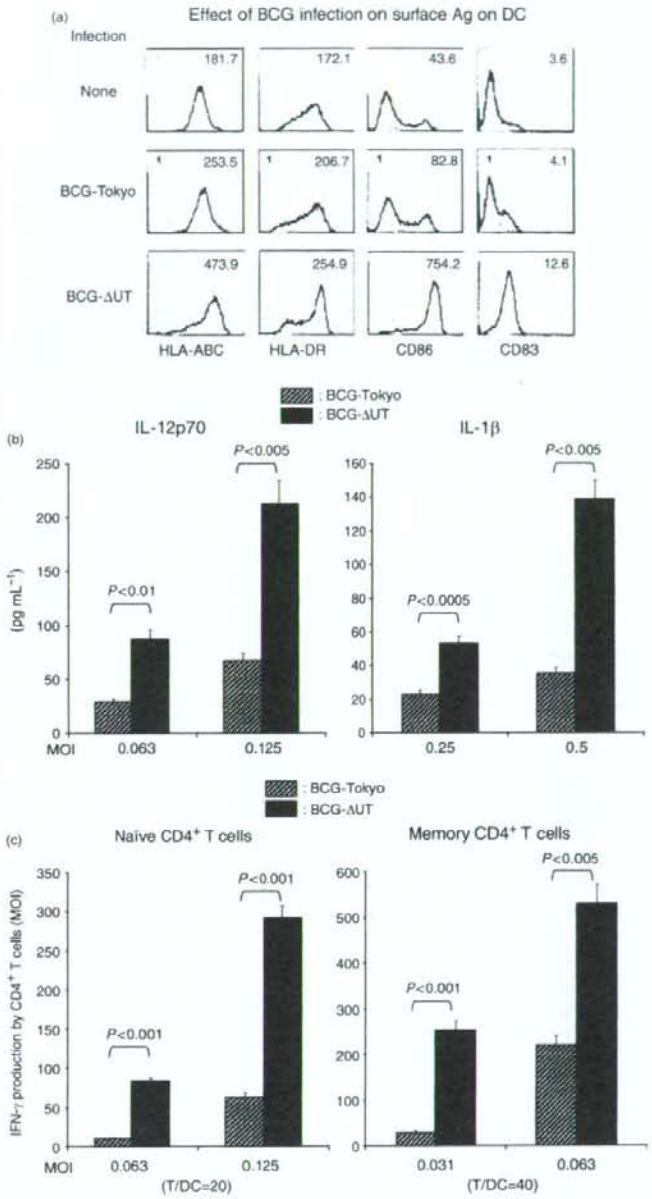

Fig. 6. (a) Expression of various molecules on BCG-infected DCs. Monocyte-derived immature DCs were infected with either BCG-Tokyo or BCG-ΔUT at an MOI of 0.25 and cultured for another 2 days in the presence of rGM-CSF and rIL-4. The DCs from day 5 were gated and analyzed. Dotted lines, isotype-matched control IgG; solid lines, the indicated test mAb. The number in the top right-hand corner of each panel represents the difference in mean fluorescence intensity between the control IgG and the test mAb. Representative results of three separate experiments are shown. (b) Cytokine production from DCs stimulated by BCG. Monocyte-derived DCs from 4 days of culture in the presence of rGM-CSF and rIL-4 were stimulated with the indicated dose of either BCG-Tokyo or BCG-ΔUT for 24 h. The concentration of the indicated cytokine was determined by the ELISA method. A representative of three separate experiments is shown. Assays were performed in triplicate and the results are expressed as the means ± SD. Titers were statistically compared using Student's *t*-test. (c) IFN-γ production by naïve CD4+ T cells and memory CD4+ T cells. DCs obtained from monocytes infected with either BCG-Tokyo or BCG-ΔUT were used as a stimulator of naïve and memory CD4+ T cells in a 4-day culture. A representative of three separate experiments is shown. Assays were performed in triplicate and the results are expressed as the means ± SD. Titers were statistically compared using Student's *t*-test.

improvement of intraphagosomal pH milieu for efficient phagosome–lysosome fusion was not sufficient for the induction of full T-cell activation as far as macrophages were concerned. Thus, we further searched for factors which might be helpful in inducing full activation of T cells. First, we examined the influence of endogenously produced IL-10, as abundant IL-10 was produced from macrophages by infection with BCG-ΔUT (data not shown). The neutralization of IL-10 from macrophages drastically enhanced T-cell activation (Fig. 3a). Furthermore, pretreatment of

© 2008 Federation of European Microbiological Societies
Published by Blackwell Publishing Ltd. All rights reserved

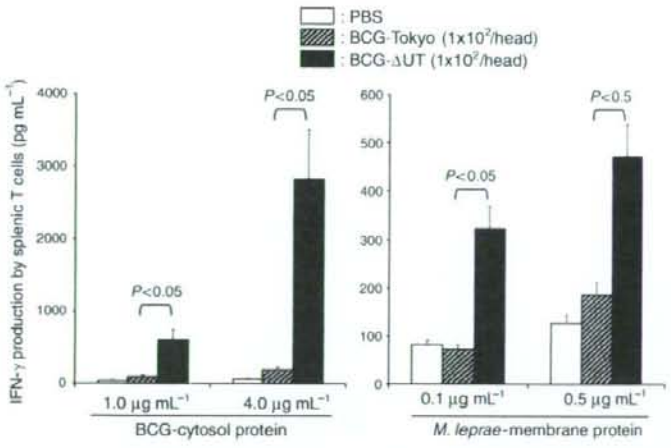

Fig. 7. IFN-γ production by splenic T cells obtained from C57BL/6 mice infected with BCG-Tokyo or BCG-ΔUT. Five-week-old C57BL/6 mice were infected with the indicated dose of BCG intradermally. Four weeks after the inoculation, splenocytes (2×10^5 cells well^{-1}) were stimulated with the indicated dose of either BCG-derived cytosol protein or *Mycobacterium leprae*-derived membrane protein for 4 days. Assays were performed in triplicate for each mouse, and the results for three mice per group are given, expressed as the means ± SD. Representative results for two separate experiments are shown. Titers were statistically compared using Student's *t*-test.

macrophages with GM-CSF, which is normally produced from activated CD4$^+$ T cells, monocytes and macrophages (data not shown), and inhibits IL-10 production (Makino *et al.*, 2007), was also quite efficient in enhancing the BCG-ΔUT-mediated T-cell activity. Therefore, the unexpectedly weak activation of CD4$^+$ T cells by BCG-ΔUT seemed to be at least partly due to the immunosuppressive effect of IL-10. Secondly, we focused on the costimulating factors capable of actively up-regulating the T-cell-stimulating function of macrophages, and found that both CD40L and IFN-γ were quite efficient. It was previously reported that both CD40L and IFN-γ were needed to costimulate macrophages infected with *M. leprae* (Makino *et al.*, 2007); however, in the present study, the sole treatment of BCG-ΔUT-infected macrophages with either CD40L or IFN-γ was enough to confer a sufficient effect (Figs 4 and 5). The high sensitivity of BCG-ΔUT-infected macrophages to CD40L may be due to the ability of rBCG to induce greater expression of CD40 (Fig. 4a). The exogenous IFN-γ may contribute to increased production of IFN-γ from T cells by activating macrophages, as it enhanced the surface expression of HLA-DR and CD86 on BCG-ΔUT-infected macrophages, which facilitated antigen-specific T-cell activation. As reported, *M. leprae* is less sensitive to IFN-γ (Makino *et al.*, 2007), and also parental BCG was found to be clearly less sensitive to IFN-γ than BCG-ΔUT. These results indicate that each mycobacterium may have differential sensitivity to IFN-γ (Verreck *et al.*, 2004). Although the molecular mechanism responsible for the difference in sensitivity remains unexplained, it is well known that IFN-γ facilitates the digestion of intracellular mycobacteria in macrophages, and thus the following speculation may be possible: in the present system, the alteration of the pH milieu of BCG-containing phagosomes caused by the depletion of urease activity may help to establish circumstances where cell activation as well as enhanced trafficking of mycobacterial antigens to the surface by the MHC class II pathway can be induced by IFN-γ treatment. The urease gene of pathogenic mycobacteria may be a good target for combination immunotherapy/chemotherapy as urease depletion downregulates the growth of mycobacteria (data not shown) and upregulates the immunoactivity of intracellular digestion of bacteria in host cells.

In contrast to macrophages, DCs were highly activated by the sole infection with BCG-ΔUT in terms of phenotype and cytokine production, and BCG-ΔUT-infected DCs efficiently activated both naïve and memory CD4$^+$ T cells in the absence of additional costimulation. The activated T cells produced abundant amounts of both IFN-γ (Fig. 5c) and GM-CSF, and induced CD40L expression (data not shown). Therefore, DCs can inherently provide the critical factors needed by BCG-ΔUT-infected macrophages. As BCG infects both macrophages and DCs *in vivo*, we evaluated the efficacy of BCG-ΔUT as a T-cell activator by using C57BL/6 mice. BCG-ΔUT was superior to BCG-Tokyo in the production of murine memory CD4$^+$ T cells, which can respond to BCG-derived recall antigen and also proteins derived from pathogenic *M. leprae*. Just 100 BCG-ΔUT bacilli were sufficient to produce such memory T cells. These findings indicate that BCG-ΔUT convincingly stimulated CD4$^+$ T cells *in vivo*. As the C57BL/6 strain is a T helper (Th)1 response-prone mouse, further study using Th2 response-prone mice would provide further insight into how memory T cells are generated by inoculation with BCG-ΔUT.

Taking our data together, BCG-ΔUT is more potent than the parental BCG in the activation of macrophages, DCs and CD4$^+$ T cells. The depletion of urease from BCG may be useful in upregulating the potency of BCG as an immunostimulator.

© 2008 Federation of European Microbiological Societies
Published by Blackwell Publishing Ltd. All rights reserved

Acknowledgements

We acknowledge the contribution of Ms N. Makino in the preparation of the manuscript. We thank Ms Y. Harada for her technical support and the Japanese Red Cross Society for kindly providing blood from healthy donors. We also thank Professor William R. Jacobs, Jr, Howard Hughes Medical Institute, for providing the plasmids, pYUB854 and phAE87. This work was supported in part by a Grant-in-Aid for Research on Emerging and Re-emerging Infectious Diseases from the Ministry of Health, Labour, and Welfare of Japan.

References

Andersen P & Doherty TM (2005) The success and failure of BCG-implications for a novel tuberculosis vaccine. *Nat Rev Microbiol* **3**: 656–662.

Bardarov S, Bardarov S Jr, Pavelka MS Jr, Sambandamurthy V, Larsen M, Tufariello J, Chan J, Hatfull G & Jacobs WR Jr (2002) Specialized transduction: an efficient method for generating marked and unmarked targeted gene disruptions in *Mycobacterium tuberculosis, M. bovis* BCG and *M. smegmatis*. *Microbiology* **148**: 3007–3017.

Charles C & Shepard MD (1960) The experimental disease that follows the injection of human leprosy bacilli into foot-pads of mice. *J Exp Med* **112**: 445–454.

Clements DL, Lee BY & Horwitz MA (1995) Purification, characterization, and genetic-analysis of *Mycobacterium tuberculosis* urease, a potentially critical determinant of host-pathogen interaction. *J Bacteriol* **177**: 5644–5652.

Dockrell HM, Young SK, Britton K *et al.* (1996) Induction of Th1 cytokine responses by mycobacterial antigens in leprosy. *Infect Immun* **64**: 4385–4389.

Dye C, Watt CJ, Bleed DM, Hosseini SM & Raviglione MC (2005) Evolution of tuberculosis control and prospects for reducing tuberculosis incidence, prevalence, and deaths globally. *JAMA* **293**: 2767–2775.

Granelli-Piperno A, Golebiowska A, Trumpfheller C, Siegal FP & Steinman RM (2004) HIV-1-infected monocyte-derived dendritic cells do not undergo maturation but can elicit IL-10 production and T cell regulation. *Proc Natl Acad Sci USA* **101**: 7669–7674.

Grode L, Seiler P, Baumann S *et al.* (2005) Increased vaccine efficacy against tuberculosis of recombinant *Mycobacterium bovis* bacille Calmette-Guérin mutants that secrete listeriolysin. *J Clin Investig* **115**: 2472–2479.

Hashimoto K, Maeda Y, Kimura H, Suzuki K, Masuda A, Matsuoka M & Makino M (2002) *Mycobacterium leprae* infection in monocyte-derived dendritic cells and its influence on antigen-presenting function. *Infect Immunity* **70**: 5167–5176.

Honerzu Bentrup K & Russell DG (2001) Mycobacterial persistence: adaptation to a changing environment [review]. *Trends Microbiol* **9**: 597–605.

Job CK (1989) Nerve damage in leprosy. *Int J Lepr Other Mycobact Dis* **57**: 532–539.

Kai M, Maeda Y, Maeda S, Fukutomi Y, Kobayashi K, Kashiwabara Y, Makino M, Abbasi MA, Khan MZ & Shah PA (2004) Active surveillance of leprosy contacts in country with low prevalence rate. *Int J Lepr Other Mycobact Dis* **72**: 50–53.

Kaufmann SHE (2005) Introduction. Rational vaccine development against tuberculosis: "those who don't remember the past are condemned to repeat it". *Microbes Infect* **7**: 897–898.

Kaufmann SHE (2006) Envisioning future strategies for vaccination against tuberculosis. *Nat Rev Immunol* **6**: 699–704.

Kaufmann SHE & McMichael AJ (2005) Annulling a dangerous liaison: vaccination strategies against AIDS and tuberculosis. *Nat Med* **11**: S33–S44.

Maeda S, Matsuoka M, Nakata N, Kai M, Maeda Y, Hashimoto K, Kimura H, Kobayashi K & Kashiwabara Y (2001) Multidrug resistant *Mycobacterium leprae* from patients with leprosy. *Antimicrob Agents Chemother* **45**: 3635–3639.

Maeda Y, Gidoh M, Ishii N, Mukai C & Makino M (2003) Assessment of cell mediated immunogenicity of *Mycobacterium leprae*-derived antigens. *Cell Immunol* **222**: 69–77.

Makino M & Baba M (1997) A cryopreservation method of human peripheral blood mononuclear cells for efficient production of dendritic cells. *Scand J Immunol* **45**: 618–622.

Makino M, Shimokubo S, Wakamatsu S, Izumo S & Baba M (1999) The role of human T-lymphotropic virus type 1 (HTLV-1)-infected dendritic cells in the development of HTLV-1-associated myelopathy/tropical spastic paraparesis. *J Virol* **73**: 4575–4581.

Makino M, Maeda Y, Fukutomi Y & Mukai T (2007) Contribution of GM-CSF on the enhancement of the T cell-stimulating activity of macrophages. *Microbes Infect* **9**: 70–77.

McDermott-Lancaster RD, Ito T, Kohsaka K, Guelpa-Lauras CC & Grosset JH (1987) Multiplication of *Mycobacterium leprae* in the nude mouse, and some applications of nude mice to experimental leprosy. *Int J Lepr Other Mycobact Dis* **55**: 889–895.

Miyamoto Y, Mukai T, Takeshita F, Nakata N, Maeda Y, Kai M & Makino M (2004) Aggregation of mycobacteria caused by disruption of fibronectin-attachment protein-encoding gene. *FEMS Microbiol Lett* **236**: 227–234.

Miyamoto Y, Mukai T, Nakata N, Maeda Y, Kai M, Naka T, Yano I & Makino M (2006) Identification and characterization of the genes involved in glycosylation pathways of mycobacterial glycopeptidolipid biosynthesis. *J Bacteriol* **188**: 86–95.

Mochida-Nishimura K, Akagawa KS & Rich EA (2001) Interleukin-10 contributes development of macrophage suppressor activities by macrophage colony-stimulating factor, but not by granulocyte-macrophage colony-stimulating factor. *Cell Immunol* **214**: 81–88.

Orme IM, Roberts AD, Griffin JP & Abrams JS (1993) Cytokine secretion by CD4 T lymphocytes acquired in response to *Mycobacterium tuberculosis* infection. *J Immunol* **151**: 518–525.

Reyrat JM, Berthet FX & Gicquel B (1995) The urease locus of *Mycobacterium tuberculosis* and its utilization for the

© 2008 Federation of European Microbiological Societies
Published by Blackwell Publishing Ltd. All rights reserved

demonstration of allelic exchange in *Mycobacterium bovis* bacillus Calmette-Guérin. *Proc Natl Acad Sci USA* **92**: 8768–8772.

Schaible UE, Sturgill-Koszycki S, Schlesinger PH & Russell DG (1998) Cytokine activation leads to acidification and increases maturation of *Mycobacterium avium*-containing phagosomes in murine macrophages. *J Immunol* **160**: 1290–1296.

Sendide K, Degmane AE, Reyrat JM, Talal A & Hmama Z (2004) *Mycobacterium bovis* BCG urease attenuates major histocompatibility complex class II trafficking to the macrophage cell surface. *Infect Immun* **72**: 4200–4209.

Setia MS, Steinmaus C, Ho CH & Rutherford GW (2006) The role of BCG in prevention of leprosy: a meta-analysis. *Lancet Infect Dis* **6**: 162–170.

Stoner GL (1979) Importance of the neural predilection of *Mycobacterium leprae* in leprosy. *Lancet* **2**: 994–996.

Verreck FA, de Boer T, Langenberg DM, Hoeve MA, Kramer M, Vaisberg E, Kastelein R, Kolk A, de Waal-Malefyt R & Ottenhoff TH (2004) Human IL-23-producing type 1 macrophages promote but IL-10-producing type 2 macrophages subvert immunity to (myco)bacteria. *Proc Natl Acad Sci USA* **101**: 4560–4565.

Wakamatsu S, Makino M, Tei C & Baba M (1999) Monocyte-driven activation-induced apoptotic cell death of human T-lymphotropic virus type I-infected T cells. *J Immunol* **163**: 3914–3919.

World Health Organization. (2006) *Fact Sheet No. 104*, Rev March, http://www.who.int/mediacentre/factsheets/fs104/en

© 2008 Federation of European Microbiological Societies
Published by Blackwell Publishing Ltd. All rights reserved

CLINICAL AND VACCINE IMMUNOLOGY, Dec. 2008, p. 1755–1759 Vol. 15, No. 12
1556-6811/08/$08.00+0 doi:10.1128/CVI.00148-08
Copyright © 2008, American Society for Microbiology. All Rights Reserved.

Serological Diagnosis of Leprosy in Patients in Vietnam by Enzyme-Linked Immunosorbent Assay with *Mycobacterium leprae*-Derived Major Membrane Protein II[▽]

Masanori Kai,[1]* Nhu Ha Nguyen Phuc,[2] Thuy Huong Hoang Thi,[2] An Hoang Nguyen,[2] Yasuo Fukutomi,[1] Yumi Maeda,[1] Yuji Miyamoto,[1] Tetsu Mukai,[1] Tsuyoshi Fujiwara,[3] Tan Thanh Nguyen,[2] and Masahiko Makino[1]

Department of Microbiology, Leprosy Research Center, National Institute of Infectious Diseases, 4-2-1 Aoba-cho, Higashimurayama, Tokyo 189-0002, Japan[1]; Quyhoa National Leprosy & Dermato-Venereology Hospital, Ghenhrang District, Quynhon City, Binhdinh, Vietnam[2]; and Institute for Natural Science, Nara University, Nara 631-8502, Japan[3]

Received 21 April 2008/Returned for modification 13 June 2008/Accepted 12 October 2008

A serological diagnostic test using phenolic glycolipid-I (PGL-I) developed in the 1980s is commercially available, but the method is still inefficient in detecting all forms of leprosy. Therefore, more-specific and -reliable serological methods have been sought. We have characterized major membrane protein II (MMP-II) as a candidate protein for a new serological antigen. In this study, we evaluated the effectiveness of the enzyme-linked immunosorbent assay (ELISA) using the MMP-II antigen (MMP-II ELISA) for detecting antibodies in leprosy patients and patients' contacts in the mid-region of Vietnam and compared to the results to those for the PGL-I method (PGL-I ELISA). The results showed that 85% of multibacillary patients and 48% of paucibacillary patients were positive by MMP-II ELISA. Comparison between the serological tests showed that positivity rates for leprosy patients were higher with MMP-II ELISA than with PGL-I ELISA. Household contacts (HHCs) showed low positivity rates, but medical staff members showed comparatively high positivity rates, with MMP-II ELISA. Furthermore, monitoring of results for leprosy patients and HHCs showed that MMP-II is a better index marker than PGL-I. Overall, the epidemiological study conducted in Vietnam suggests that serological testing with MMP-II would be beneficial in detecting leprosy.

Leprosy is a chronic infectious disease caused by *Mycobacterium leprae* infection, which sometimes leads to progressive peripheral nerve injury and systematic deformity (16, 30). Early detection of *M. leprae* infection and early start of treatment are key in avoiding deformities. Also, in order to decrease the incidence of new cases, it is important to find and treat the sources of the infection as soon as possible. Thus, early detection of these infected individuals who cannot be clinically diagnosed is critical (34). The diagnosis of leprosy is based on microscopic detection of acid-fast bacilli in skin smears or biopsies, along with clinical and histopathological evaluation of suspected patients. Recently, diagnostic methods for leprosy based on *M. leprae* DNA sequences have been developed (10, 20, 25). However, it is difficult to use these methods in developing countries which still have leprosy hot spot areas, because such methods require expensive machines and materials as well as skilled technicians. Although many developing countries have recently established laboratories for DNA-based diagnosis, it is harder to perform DNA tests than serodiagnostic tests. Thus, in countries where leprosy is endemic, diagnosis still relies on clinical observations and easy, inexpensive tests.

Serodiagnosis is generally accepted as the easiest way of diagnosing a disease. For leprosy serodiagnosis, the only antigen currently used is phenolic glycolipid I (PGL-I), which is supposedly specific to *M. leprae* (21, 26, 27). Since the identification of PGL-I in 1981 by Hunter and Brennan (14), a number of serological tools have been developed. Simple assays, such as the Serodia-Leprae method, a dipstick assay, and lateral flow tests based on the PGL-I antigen, have been used to detect leprosy patients in areas where leprosy is endemic (3, 15, 17, 32). However, these tests seem to be insufficient for detection of both multibacillary (MB) and paucibacillary (PB) patients, as well as for early diagnosis, and have not been used as widely as would be expected in field situations (6, 29). Therefore, we have begun the search for a more sensitive antigen. Major membrane protein II (MMP-II; encoded by the ML2038c gene, named *bfrA*, also known as bacterioferritin) was previously identified from the cell membrane fraction of *M. leprae* as an antigenic molecule capable of activating both antigen-presenting cells and T cells (19, 24). A homology search of the mycobacteria nucleotide database revealed that MMP-II is conserved between *M. leprae*, *M. tuberculosis*, and *M. avium*. The amino acid identity is about 86% among the three species. However, we have previously examined the role of MMP-II in the humoral responses of Japanese patients and showed that MMP-II could contribute to the specific serodetection of leprosy patients (18).

In the present study, we performed a serological test using serum samples collected in regions of leprosy endemicity in Vietnam and evaluated the use of MMP-II as an antigen for serodiagnosis of leprosy. We believe that identifying the appropriate antigens for serodiagnosis could facilitate the devel-

* Corresponding author. Mailing address: Department of Microbiology, Leprosy Research Center, National Institute of Infectious Diseases, 4-2-1 Aoba-cho, Higashimurayama, Tokyo 189-0002, Japan. Phone: 81-42-391-8211. Fax: 81-42-391-8807. E-mail: mkai@nih.go.jp.
▽ Published ahead of print on 22 October 2008.

opment of simple diagnostic tests, like dip-stick assays, for use in developing countries.

MATERIALS AND METHODS

Serum samples. A total of 974 serum samples from various individuals, including in- and out-patients of Quyhoa National Leprosy & Dermato-Venereology Hospital (NDH), were obtained under informed consent. The sera were donated by 205 leprosy patients (163 patients undergoing treatment and 42 new patients), 428 household contacts (HHCs), 130 medical staff members, and 211 noncontact healthy individuals. Sera of leprosy patients and their contacts were taken at regional medical centers in the midregion of Vietnam, including those in the Danang, Quangnam, Quangngai, Binhdinh, Phuyen, Khanhhoa, Ninhthuan, Gialai, Kontum, Daklak, and Daknong provinces, where the average prevalence rate is 0.17 (number of cases/10,000 persons) and the average detection rate is 2.13 (number of cases/10,000 persons). Among these provinces, Binhdinh, Ninhthuan, Gialai, and Kontum had hot spot areas. The medical staff members consisted of workers in Quyhoa NDH, including medical doctors, nurses, pharmacists, technicians, and helpers. Only the sera from medical staff members who were not HHCs of leprosy patients were used in this study. Sera were also obtained from healthy persons living in the Binhdinh province (n = 126) and the Longan province (n = 85), which are distantly located from each other. Out of 205 leprosy patients, 121 had MB leprosy and 84 had PB leprosy. We made the initial diagnosis according to the Ridley-Jopling classification system and classified patients as MB and PB types based on the WHO recommendation. In Vietnam, the *M. bovis* bacille Calmette-Guérin (BCG) vaccination against tuberculosis has been undertaken in earnest since 1976. Almost all medical staff personnel who donated their blood for this study were vaccinated with BCG.

MMP-II and PGL-I antigens. The MMP-II gene (ML2038c, or *bfrA*) was expressed in *Escherichia coli* as a fusion construct by using a pMAL-c2X expression vector (New England BioLabs) (18). Synthetic bovine serum albumin-conjugated trisaccharide-phenyl propionate for the detection of PGL-I antibodies was produced by our laboratory. The procedure for synthesis of the antigen is described elsewhere (12).

ELISAs for detection of antibodies. MaxiSorp (Nalge Nunc) microtiter plates were coated with 50 μl antigen solution (MMP-II [0.4 μg/ml] and PGL-I [0.2 μg/ml]) in carbonate-bicarbonate buffer (pH 9.4) and kept at 4°C overnight. The optimal concentrations of these antigens were determined in advance. The enzyme-linked immunosorbent assay (ELISA) protocol was performed as described previously (18). We measured anti-MMP-II immunoglobulin G (IgG) antibodies and anti-PGL-I IgM antibodies. Plate-to-plate variations in optical density (OD) readings were controlled for by using a common standard serum.

Monitoring. One hundred forty-eight leprosy patients have been monitored using MMP-II ELISA and PGL-I ELISA during their multidrug therapy (MDT) treatment since 2001. Twelve-month MDT for MB was carried out, and sampling was performed three to five times. Also, HHCs were monitored once every 3 or 6 months by both the MMP-II and the PGL-I ELISA methods from 2001 to 2004.

Statistics. The data were analyzed using a statistical software package (version 9.3.2.0; MedCalc software). A receiver operator characteristic (ROC) curve was drawn to calculate the cutoff levels (2). Additionally, the statistically significant differences between assays were confirmed by the chi-square test (28).

RESULTS

Comparison of the distribution of ELISA values between MMP-II and PGL-I. We focused on the distribution of ELISA values derived from MB leprosy patients and compared them to those from healthy individuals (Fig. 1). The cutoff OD_{405} value for anti-MMP-II antibody was defined as 0.103 (95% confidence interval, 85.2 to 93.7), and that for anti-PGL-I antibody was defined as 0.452 (95% CI, 85.2 to 93.7), by ROC curve analysis (MedCalc software) using OD titers from 211 healthy individuals and 205 leprosy patients. The distribution pattern of MMP-II ELISA values was quite different from that of PGL-I ELISA for healthy individuals. While the OD values of most healthy individuals were in the low range for MMP-II ELISA (Fig. 1A), the titers obtained by PGL-I ELISA showed a bell-shaped curve which was similar to that of MB leprosy patients (Fig. 1B). The PGL-I ELISA values for PB leprosy patients also showed a similar bell-shaped curve (data not shown).

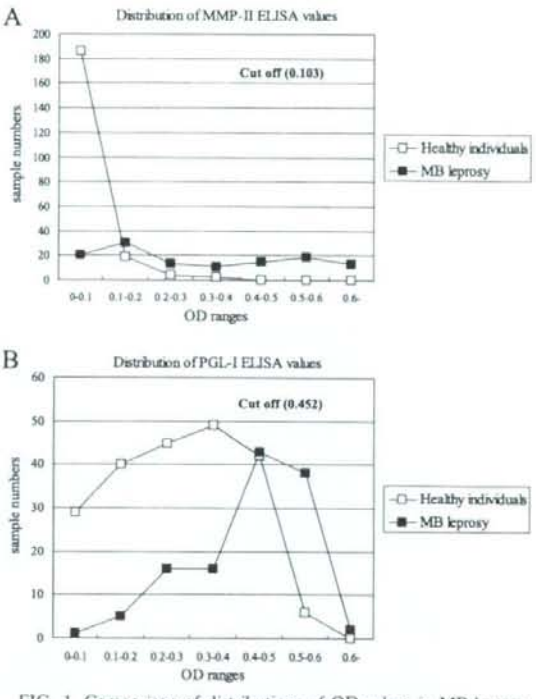

FIG. 1. Comparison of distributions of OD values in MB leprosy patients and normal individuals. (A) Distribution pattern of MMP-II ELISA values in patients and healthy individuals. (B) Distribution pattern of PGL-I ELISA values in patients and healthy individuals. The solid squares show the number of MB leprosy patients in each OD value range, and the open squares show the number of healthy individuals.

Detection rate of antibodies in sera of leprosy patients. Among the MB patients, 85.1% were positive by MMP-II ELISA and 57.0% were positive by PGL-I ELISA; 47.6% of PB patients were positive by MMP-II ELISA, and 20.2% were positive by PGL-I ELISA (Fig. 2). The MMP-II ELISA values for both MB and PB patients were significantly higher than the PGL-I ELISA values ($P < 0.001$) (Fig. 2). Patients undergoing treatment and new cases showed a similar difference (data not shown).

Seropositivity rates of contacts, medical staff members, and healthy volunteers. There was no significant difference in positivity rate between MMP-II ELISA and PGL-I ELISA for healthy individuals and HHCs (Fig. 3). Also, there was no significant difference in positivity rate between MMP-II ELISA and PGL-I ELISA for healthy individuals from different provinces, namely, Binhdinh and Longan (data not shown). In contrast, the medical staff showed a significantly higher rate of positivity by MMP-II ELISA (26.2%) than by PGL-I ELISA. The anti-MMP-II antibody positivity rate for the medical staff